This journal is © The Royal Society of Chemistry 2013

Supplementary material to Ewald et al.

Table S1 – List of genes included in this study

All *S. cerevisiae* deletions were introduced into a prototrophic CEN.PK background strain by replacement with the kanMX4 or the natNT2 cassette [a]by Blank et al.[1] or [b]in this study. [c]not included in original screen

mutant	alias	ORF
WT	CEN.PK 113-7D haploid mat α	
ADH1[a]	*ADC1*	YOL086C
ADH3[a]	-	YMR083W
ALD5[a]	-	YER073W
ALD6[a]	*ALD1*	YPL061W
COX5a[a]	-	YNL052W
CTP1[a]	-	YBR291C
DAL7[a]	*MLS2, MSL2*	YIR031C
FUM1[a]	-	YPL262W
GCV2[a]	*GSD2*	YMR189W
GLY1[a]	-	YEL046C
GND2[a]	-	YGR256W
ICL1[a]	-	YER065C
IDP1[a]	-	YDL066W
IDP2[a]	-	YLR174W
LSC1[a]	-	YOR142W
MAE1[a]	-	YKL029C
MDH1[a]	-	YKL085W
MDH2[a]	-	YOL126C
MDH3[a]	-	YDL078C
MLS1[a]	-	YNL117W
NQM1[a]	-	YGR043C
OAC1[a]	-	YKL120W
PCK1[a]	*JPM2, PPC2*	YKR097W
PGM1[a]	-	YKL127W
PGM2[a]	*GAL5*	YMR105C
SDH1[a]	-	YKL148C
SER33[a]	-	YIL074C
SFC1[a]	*ACR1*	YJR095W
SOL1[a]	-	YNR034W
SOL2[a]	-	YCR073W-A
SOL3[a]	-	YHR163W
SOL4[a]	-	YGR248W
TAL1[a]	-	YLR354C
TAL1, NQM1[b,c]		
TKL1[b]	-	YPR074C

Reference:
Blank, L.M., Küpfer, L. & Sauer, U. Large-scale ^{13}C-flux analysis reveals mechanistic principles of metabolic network robustness to null mutations in yeast. *Genome Biol* **6**, R49 (2005)

This journal is © The Royal Society of Chemistry 2013

Table S2 - Quantitative metabolomics: analytical platforms and internal standards

Two different platforms were used for metabolite measurements, GC-TOF and LC-MS/MS (as described in Materials and Methods). Listed are the name as used in the main text and figures, the full name and the Pubchem/CHEBI ID. As internal standards for quantification, we used labeled biomass (13CbM) for the LC and norvaline (nval) or glutarate (glut) for the GC, respectively, as indicated in column 5. * >90 % 3 PG in samples

name	full name	Pubchem ID	platform	internal standard
BPG	bisphosphoglycerate	61+683	LC-MS/MS	13Cbm
2PG+3PG*	3-phosphoglycerate	59 + 439183	LC-MS/MS	13Cbm
6PG	6-phosphogluconolactone	91493	LC-MS/MS	13Cbm
ADP	adenosine-diphosphate	6022	LC-MS/MS	13Cbm
a-ketoglutarate/ αKG	alpha-ketoglutarate	51	GC	glut
alanine		5950	GC	nval
AMP	adenosine-monophosphate	6083	LC	13Cbm
arginine		232	LC	13Cbm
asparagine		236	GC	nval
aspartate		424	GC	nval
ATP	adenosine-triphosphate	5957	LC	13Cbm
citrate		311	GC	glut
DHAP	dihydroxyacetone-phosphate	4643300	LC	13Cbm
disaccharides	trehalose + maltose	1143+6255	LC	13Cbm
E4P	erythrose-4-phosphate	122357	LC	13Cbm
F1P	fructose-1-phosphate	65246	LC	13Cbm
F6P+G1P	fructose-6-phosphate glucose-1-phosphate	69507+65533	LC	13Cbm

This journal is © The Royal Society of Chemistry 2013

name	full name	Pubchem ID	platform	internal standard
fumarate		723	GC	Glut
G6P	glucose-6-phosphate	99058	LC	13Cbm
glutamate		611	GC	nval
glutamine		738	GC	nval
glycine		752	GC	nval
GTP	guanosine-triphosphate	762	LC	13Cbm
homoserine		12647	GC	nval
isocitrate		1198	GC	glut
isoleucine		6306	GC	nval
leucine		6106	GC	nval
lysine		5962	GC	nval
malate		525	GC	glut
methionine		6137	GC	nval
NAD	nicotineamidedinucleotide, oxidized	925	LC	13Cbm
NADH	nicotineamiddinucleotide, reduced	928	LC	13Cbm
NADP	nicotineamiddinucleotide-phosphate, oxidized	4412	LC	13Cbm
ornithine		6262	GC	nval
PEP	phospho-enolpyruvate	1005	LC	13Cbm
phenylalanine		994	GC	nval
proline		145742	GC	nval
R1P	ribose-1-phosphate	439236	LC	13Cbm
R5P	ribose-5-phosphate	77982	LC	13Cbm

This journal is © The Royal Society of Chemistry 2013

name	full name	Pubchem ID	platform	internal standard
Ru5P+Xu5P	ribulose- and xylulose-5-phosphate	850	LC	13Cbm
S7P	seduheptulose-7-phosphate	165007	LC	13Cbm
serine		5951	GC	nval
shikimate		1094	LC	13Cbm
succinate		1110	GC	glut
threonine		6288	GC	nval
tryptophane		1148	GC	nval
tyrosine		1153	GC	nval
valine		6287	GC	nval

Table S3 - Growth rates of 33 *S. cerevisiae* mutants on three different carbon substrates.

Growth rates are given as ratios to the wild type (WT) growth rate on the same substrate. n=4, standard deviations were generally below 10 %. The specific growth rate of the wild type on glucose, galactose, and ethanol was 0.38, 0.12, and 0.15 h^{-1}, respectively. NG = no detectable growth in liquid media within 48 h. *growth in these mutants was so severely reduced (< 0.01 h^{-1}) that a precise measurement was not possible. These were omitted from metabolome analysis because of the impossibility to produce sufficient biomass.

mutant	Relative growth rate		
	glucose	galactose	ethanol
WT	1.00	1.00	1.00
SOL4	1.02	1.04	1.03
CTP1	1.00	1.03	0.98
LSC1	1.00	1.09	0.90
MAE1	1.00	1.15	0.68
SDH1	0.99	<0.1*	NG
MDH2	0.99	1.03	NG
PGM2	0.99	0.32	0.94
SER33	0.97	0.87	0.99
GND2	0.97	1.01	0.96
IDP1	0.96	0.88	0.91
ALD5	0.96	0.95	0.96
SOL2	0.95	1.07	0.93
DAL7	0.95	0.92	0.97
SOL1	0.94	0.99	0.97
MLS1	0.94	1.01	NG
PCK1	0.94	0.99	NG
NQM1	0.93	1.00	0.97
GCV2	0.92	0.99	NG
IDP2	0.92	1.10	0.79
MDH3	0.91	0.99	0.85
ICL1	0.91	1.07	NG
ADH3	0.91	0.96	0.97
GLY1	0.90	0.97	0.91
SFC1	0.87	0.93	NG
MDH1	0.86	1.08	NG
TAL1	0.86	1.05	0.97
PGM1	0.84	NG	1.00
ALD6	0.78	0.99	0.64
OAC1	0.75	1.09	0.88
SOL3	0.66	1.00	0.97
COX5a	0.62	<0.1*	NG
FUM1	0.47	NG	NG
ADH1	0.47	0.95	0.94
TKL1	NG	NG	NG

Table S4 – Mass action ratios

To systematically check for shift in chemical equilibrium around enzymes, we calculated pseudo mass action ratios for reactions in primary metabolism according to the stoichiometry defined below. Reactions were lumped if intermediates could not be measured. Cofactors were omitted from the analysis because of their homeostatic behavior.

name	enzymes involved	assumed stoichiometry
PGI	Pgi1	[F6P+G1P]/[G6P]
PGM	Pgm1/Pgm2	[G6P] /[F6P+G1P]
PFK	Pfk1/Pfk2	[FBP]/[G6P]
FBA	Fba1+Tpi1	[DHAP]*[DHAP]/[FBP]
TDH	Tpi1+Tdh1/Tdh2/Tdh3	[BPG]/[DHAP]
PGK	Pgk1	[3PG]/[BPG]
ENO	Gpm1/Gpm2+Eno1/Eno2	[PEP]/[3PG]
TCAin	Pyk1/Pyk2+Pda1/Pdb1+Cit1/Cit2/ Cit3 +Mdh1/Mdh2/Mdh3	[citrate]/[PEP]*[malate]
ACO	Aco1/Aco2	[isocitrate]/[citrate]
IDH	Idh1/Idh2	[α-ketoglutarate]/[isocitrate]
LSC	Kgd1+Kgd2+Lsc1/Lsc2	[succinate]/[α-ketoglutarate]
SDH	Sdh1+Sdh2+Sdh3+Sdh4	[fumarate]/[succinate]
FUM	Fum1	[malate]/[fumarate]
MAE	Mae1+Pyk1/Pyk2	[malate]/[PEP]
ICL	Icl1/Icl2	[succinate]/[isocitrate]
OxPPP	Zwf1+Sol3/Sol4	[6PG]/[G6P]
GND	Gnd1/Gnd2	[Ru5P+Xu5P]/[6PG]
RKI	Rki1	[R5P]/ [Ru5P+Xu5P]
TKLa	Tkl1/Tkl2+Tpi1	[DHAP]*[S7P]/ [Ru5P+Xu5P]*[R5P]
TKLb	Tkl1/Tkl2+Tpi1	[DHAP]*[F6P+G1P]/[Ru5P+Xu5P]*[E4P]
TAL	Tal1/Nqm1+Tpi1	[DHAP]*[S7P]/[E4P]*[F6P+G1P]
GDH	Gdh1/Gdh2/Gdh3	[glutamate]/[α-ketoglutarate]
GLN	Gln1	[glutamine]/[glutamate]

Table S5 - Adenylate energy charge

Adenylate energy charge (Atkinson et al.) of the 33 deletion strains on three different substrates, calculated as
AEC= ([ATP]+0.5*[ADP])/([ATP]+[ADP]+[AMP])

	adenylate energy charge (AEC)					
	glucose		**galactose**		**ethanol**	
mutant	**average**	**s.d.**	**average**	**s.d.**	**average**	**s.d.**
WT	0.91	± 0.01	0.89	± 0.02	0.76	± 0.10
ADH1	0.81	± 0.10	0.86	± 0.00	0.80	± 0.03
ADH3	0.91	± 0.01	0.88	± 0.02	0.82	± 0.01
ALD5	0.89	± 0.02	0.87	± 0.03	0.82	± 0.05
ALD6	0.90	± 0.02	0.89	± 0.00	0.83	± 0.04
COX5a	0.87	± 0.09				
CTP1	0.90	± 0.02	0.88	± 0.02	0.77	± 0.09
DAL7	0.90	± 0.02	0.89	± 0.02	0.81	± 0.06
FUM1	0.92	± 0.03				
GCV2	0.91	± 0.03	0.88	± 0.01	0.88	± 0.01
GLY1	0.90	± 0.01	0.88	± 0.02	0.84	± 0.04
GND2	0.89	± 0.03	0.88	± 0.02	0.80	± 0.04
ICL1	0.91	± 0.03	0.89	± 0.02	0.89	± 0.02
IDP1	0.89	± 0.01	0.89	± 0.02	0.84	± 0.04
IDP2	0.89	± 0.02	0.89	± 0.02	0.80	± 0.03
LSC1	0.89	± 0.03	0.89	± 0.02	0.83	± 0.03
MAE1	0.90	± 0.01	0.90	± 0.01	0.80	± 0.02
MDH1	0.91	± 0.01	0.87	± 0.03	0.87	± 0.03
MDH2	0.89	± 0.04	0.87	± 0.02	0.87	± 0.02
MDH3	0.89	± 0.03	0.89	± 0.01	0.82	± 0.01
MLS1	0.93	± 0.03	0.85	± 0.02	0.85	± 0.02
NQM1	0.91	± 0.01	0.88	± 0.03	0.77	± 0.08
OAC1	0.90	± 0.02	0.88	± 0.01	0.77	± 0.06
PCK1	0.92	± 0.01	0.90	± 0.01	0.90	± 0.01
PGM1	0.91	± 0.02			0.79	± 0.06
PGM2	0.89	± 0.03	0.88	± 0.03	0.78	± 0.06
SDH1	0.89	± 0.03				
SER33	0.90	± 0.03	0.88	± 0.02	0.84	± 0.01
SFC1	0.90	± 0.00	0.90	± 0.01	0.90	± 0.01
SOL1	0.90	± 0.02	0.89	± 0.01	0.82	± 0.03
SOL2	0.91	± 0.02	0.87	± 0.04	0.82	± 0.06
SOL3	0.94	± 0.01	0.88	± 0.01	0.76	± 0.07
SOL4	0.89	± 0.01	0.88	± 0.04	0.82	± 0.05
TAL1	0.90	± 0.03	0.88	± 0.01	0.82	± 0.05

Reference:

Atkinson, D. E. Energy charge of the adenylate pool as a regulatory parameter. Interaction with feedback modifiers. *Biochemistry* **7**, 4030-4034 (1968).

Table S6 – Growth and metabolic phenotype for isoenzyme knockouts.

Growth phenotypes are based on the measured growth rates reported in Supplementary Table 3. Metabolic phenotypes were evaluated from metabolome measurements (Supplementary Data). ND, known isoenzymes that were not included in this study. *, mitochondrial.

	glucose		**galactose**		**ethanol**	
	growth	metabolic	growth	metabolic	growth	metabolic
Alcohol dehydrogenase						
ADH1	**-50%**	**global**	silent	**local**	silent	silent
*ADH3**	silent	silent	silent	silent	silent	silent
ADH2,4,5,6	ND					
Aldehyde dehydrogenase						
*ALD5**	silent	silent	silent	silent	silent	silent
ALD6	**-20%**	**local**	silent	silent	**-35%**	silent
*ALD1-4**	ND					
6-phosphogluconate dehydrogenase						
GND1	**lethal**	-	**lethal**	-	**lethal**	-
GND2	silent	silent	silent	silent	silent	silent
Malate synthase						
DAL7	silent	silent	silent	silent	silent	silent
MLS1	silent	silent	silent	**local**	**lethal**	
Isocitrate dehydrogenase						
*IDP1**	silent	silent	silent	**local**	silent	silent
IDP2	silent	silent	silent	silent	**-20%**	silent
IDP3	ND					
Malate dehydrogenase						
*MDH1**	**-15%**	**local**	silent	**local**	**lethal**	-
MDH2	silent	silent	silent	silent	**lethal**	-
MDH3	silent	silent	silent	silent	**-15%**	silent
Transaldolase						
TAL1	**-15%**	**local**	silent	silent	silent	silent
NQM1	silent	silent	silent	silent	silent	silent
Phosphogluco mutase						
PGM1	**-15%**	**local**	lethal	-	silent	silent
PGM2	silent	silent	**-70%**	**local**	silent	silent
6-phosphoglucono lactonase						
SOL1	silent	silent	silent	silent	silent	silent
SOL2	silent	silent	silent	silent	silent	silent
SOL3	**-35%**	**local**	silent	**local**	silent	silent
SOL4	silent	silent	silent	silent	silent	silent

Figure S1 – Metabolic network of central carbon metabolism in *S. cerevisiae* and genes included in this study.

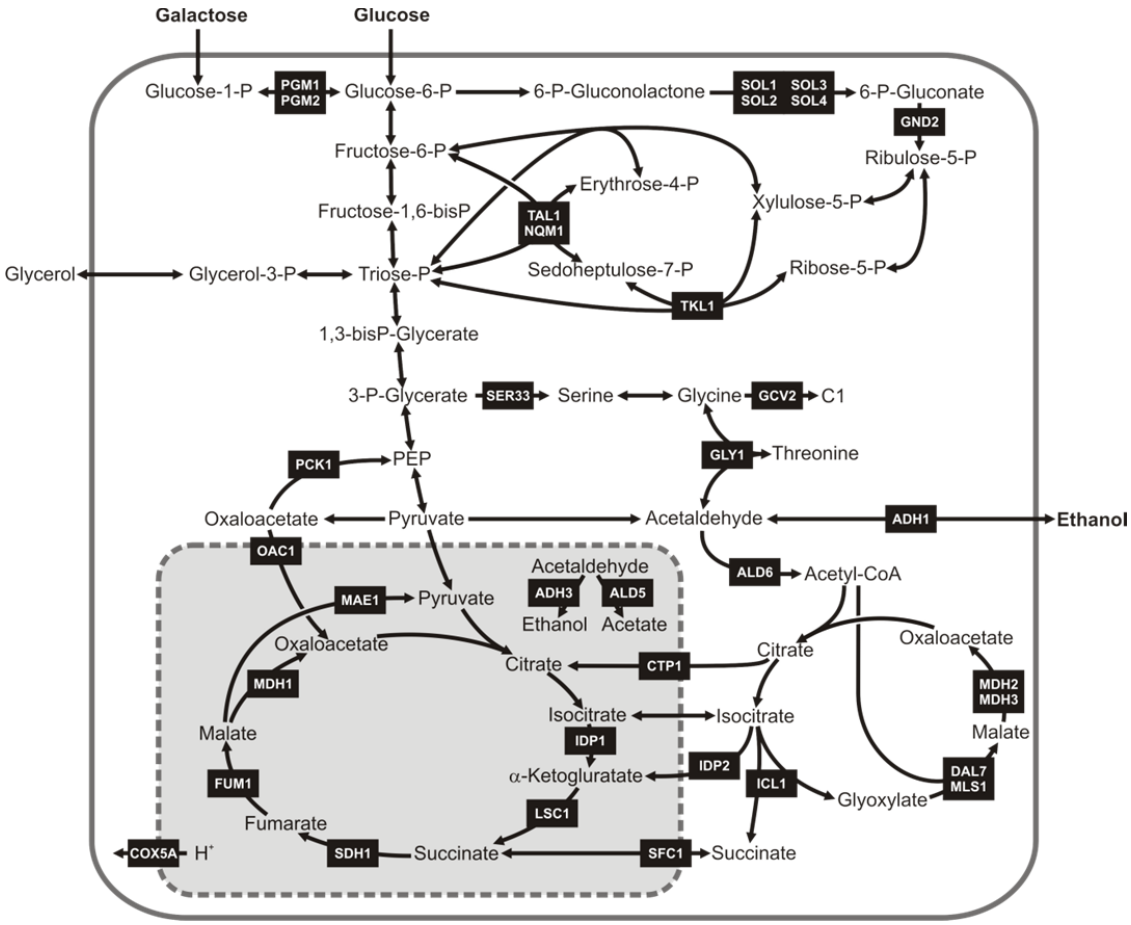

Figure S2 – Correlation analysis between growth rate and metabolome.

(A) Relative metabolite concentrations of healthy (solid symbols) and sick (open symbols) mutants on glucose (red), galactose (green), and ethanol (blue). All mutants with a reduction in growth of 30% or more were flagged as sick. For each metabolite and substrate, the concentrations in the mutants were normalized to that of the wild-type. In the case of glucose, only 1,3-BiP-Glycerate (BPG, marked with *) was found to be different (two-tailed t-test, $p < 10^{-4}$). The number of sick individuals on galactose and ethanol does not allow statistical testing.
(B) Mutual information content calculated between all metabolites and the relative growth rate (normalized to that of the wild-type, cfr. Supplementary Table 2). The value was calculated according to Peng et al. either individually for the three substrates (n = 34, 30, and 24) or for cases simultaneously (n = 88). Note that to emphasize differences between generally very low scores, the color scaling covers only the bottom 10% of the possible range (maximum = 1). The highest value was found for glutamate in the glucose case and equals 0.09 (Pearson correlation coefficient = -0.08). Overall, we conclude that no relevant correlation exists between any of the measured metabolites and growth rate.

Reference:

Peng, H., Long, F. & Ding, C. Feature selection based on mutual information: criteria of max-dependency, max-relevance, and min-redundancy. *IEEE Transactions on Pattern Analysis and Machine Intelligence* **27**, 1226-1238 (2005).

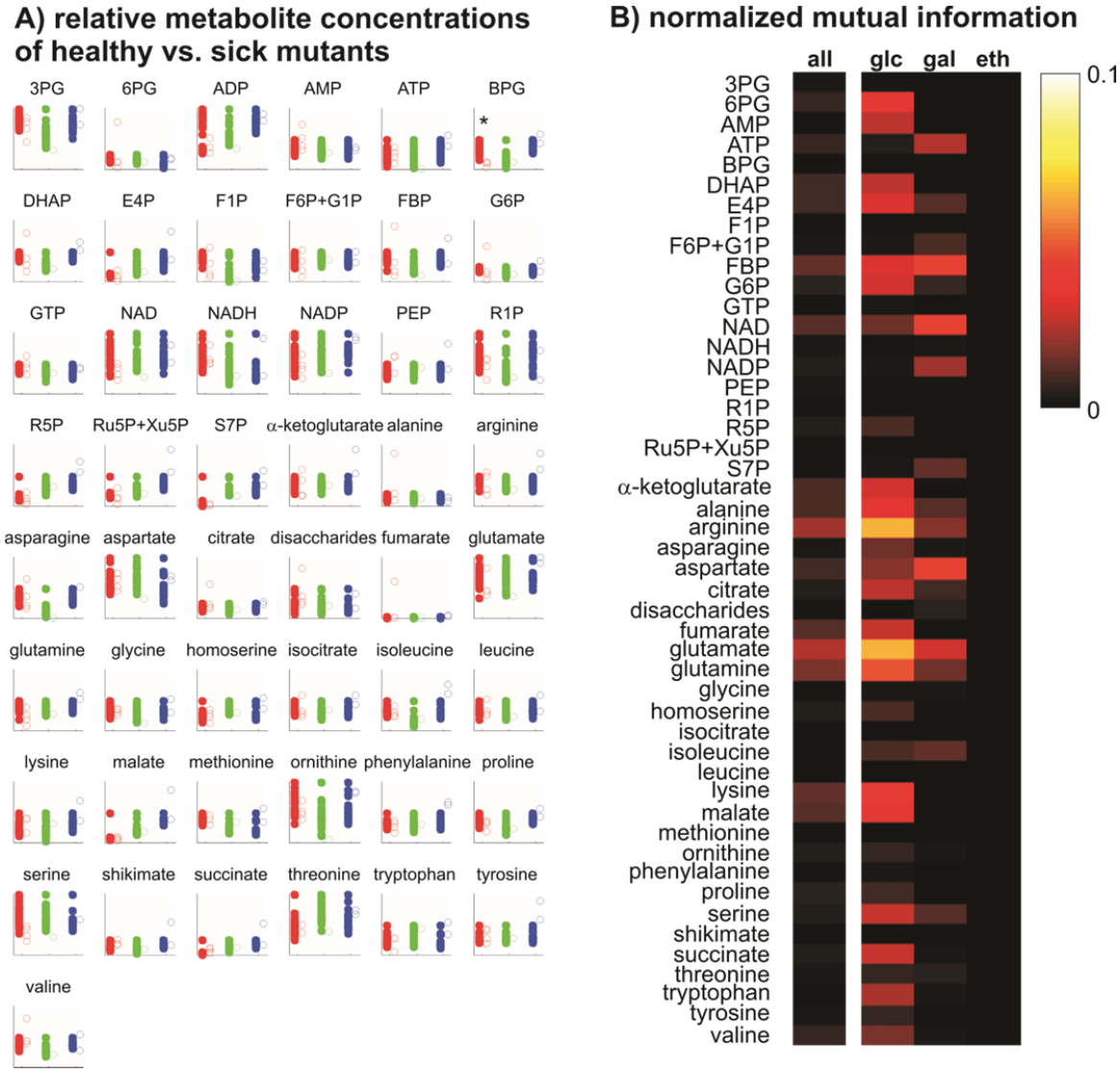
A) relative metabolite concentrations of healthy vs. sick mutants
3PG
6PG
ADP
AMP
ATP
BPG
*
DHAP
E4P
F1P
F6P+G1P
FBP
G6P
GTP
NAD
NADH
NADP
PEP
R1P
R5P
Ru5P+Xu5P
S7P
α-ketoglutarate
alanine
arginine
asparagine
aspartate
citrate
disaccharides
fumarate
glutamate
glutamine
glycine
homoserine
isocitrate
isoleucine
leucine
lysine
malate
methionine
ornithine
phenylalanine
proline
serine
shikimate
succinate
threonine
tryptophan
tyrosine
valine
B) normalized mutual information
all
glc
gal
eth
0.1
0

Figure S3 – Correlation between metabolite concentrations and metabolic fluxes.

With a dataset of 33 mutants growing on glucose, Pearson correlation coefficients were calculated between the average metabolite pools measured in this study and the metabolic fluxes determined experimentally by 13C-tracer experiments (Blank et al.). For graphic purposes, metabolites and fluxes were clustered using Euclidean distance.

The largest correlation (~ 0.5) could be found between fumarate and the C4-moiety of the tricarboxylic acid cycle. Most correlations are in the range of -0.3 – +0.3, thus pointing to a generally poor relationship between metabolites and fluxes.

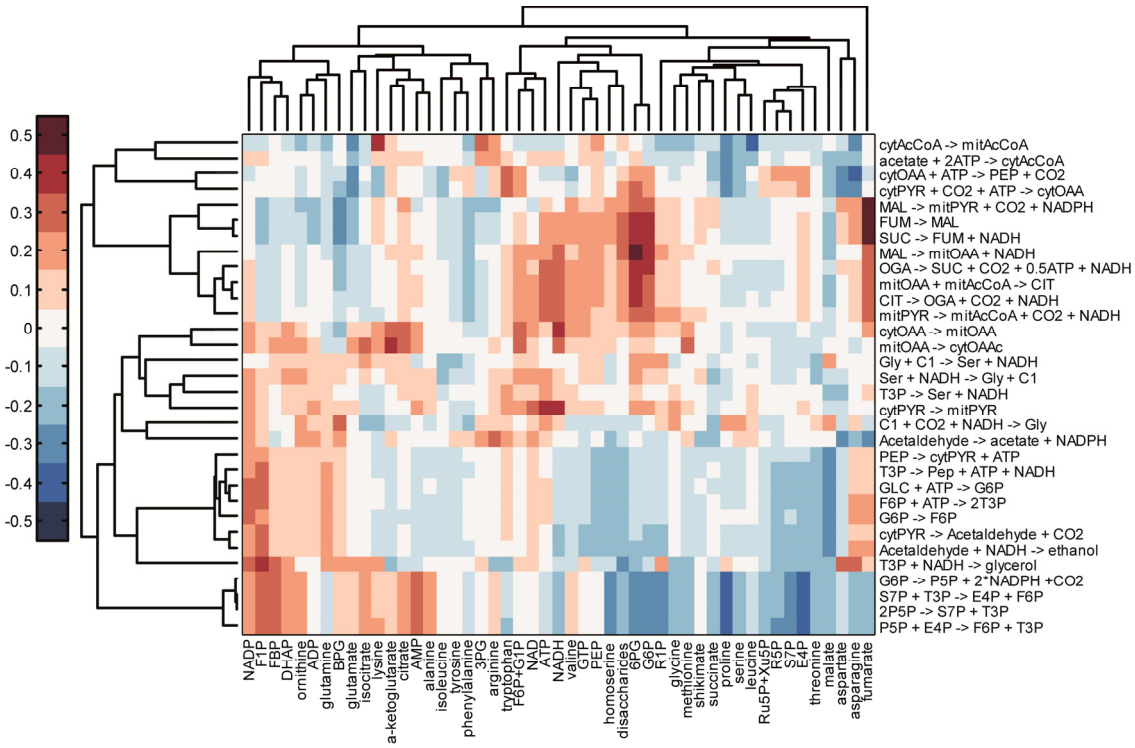

References:

Blank, L.M., Küpfer, L. & Sauer, U. Large-scale 13C-flux analysis reveals mechanistic principles of metabolic network robustness to null mutations in yeast. Genome Biol 6, R49 (2005).

Figure S4 – Multivariate analysis of metabolome data

To rank the effects of environment and mutations on the metabolome, we performed a principal component analysis with the average metabolite concentrations measured in at least four biological replicates during exponential grow on minimal medium with either glucose (red), galactose (green), or ethanol (blue). To compensate for the heterogeneous abundance of metabolites in vivo, all concentrations of each compound were first standardized to mean 0 and variance 1. The initial two principal components account for 95% of the total variance and fully discriminate between substrates, whilst the different mutants on one substrate cluster together (A). The corresponding coefficients are shown in (B). The dominating role of the substrate is independently confirmed by hierarchical clustering (C) after standardization of concentrations.

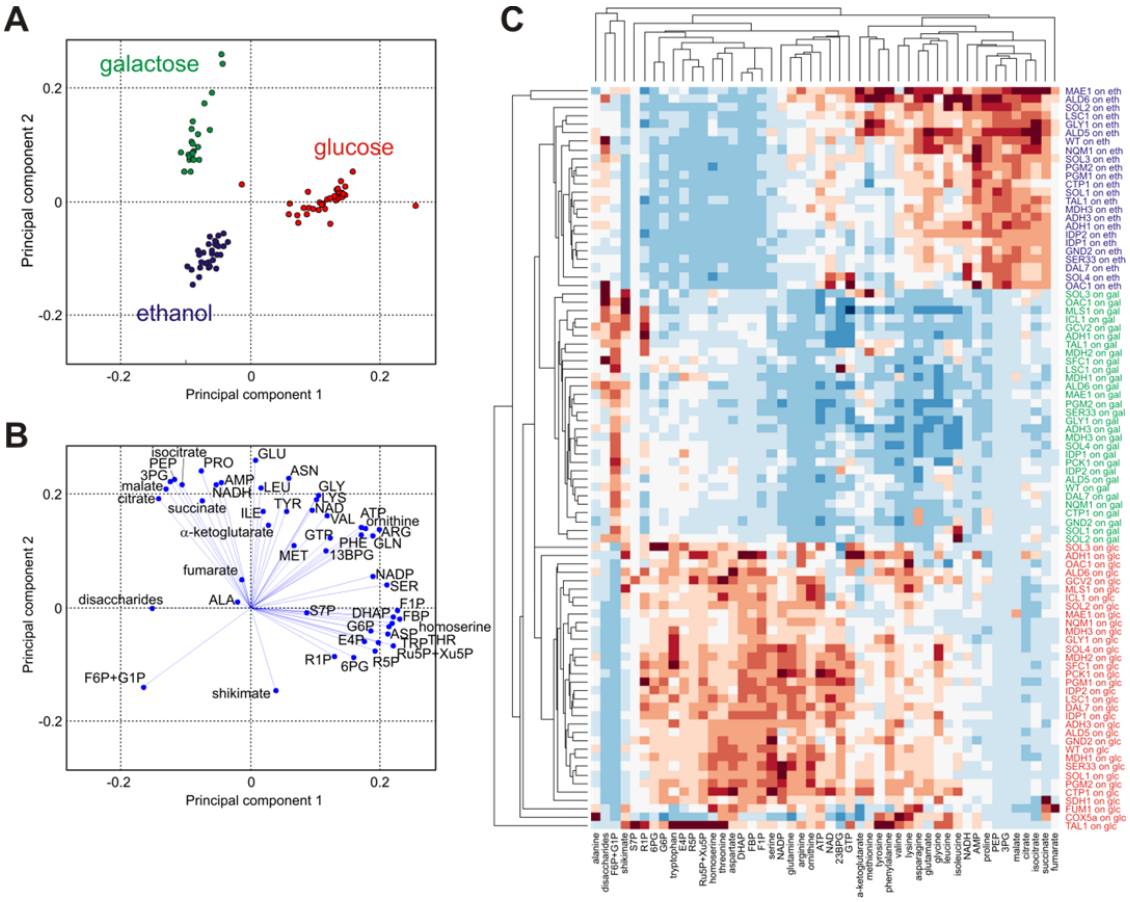

This journal is © The Royal Society of Chemistry 2013

Figure S5 – Analysis of changes in chemical equilibrium in enzymatic mutants.

For the list of reactions involved in central carbon metabolism (see Supplementary Table 4 for details), we calculated the change in mass action (MA) ratios compared to the reference state of the wild type. Down-regulation of an enzyme is expected to produce an accumulation of its substrates and, thus, a decrease in mass action ratio and a blue color in the plot. The color scaling was changed to emphasize small changes. The largest fold-change is -8.7 (log2) for the FUM reaction in the *FUM1* deletion on glucose. In general, the strongest effects on the metabolome are observed immediately upstream the delete enzyme. Only in the case of growth-deficient strains (marked with an asterisk *), distributed effects can be seen. On galactose, the apparently high scores of *MLS1*, *NQM1*, and *ICL1* mutants for the reactions TDH, PGK, TKLa, TAL are caused by the noisy measurement of glyceraldehyde-3-phosphate.

(figure on next page)

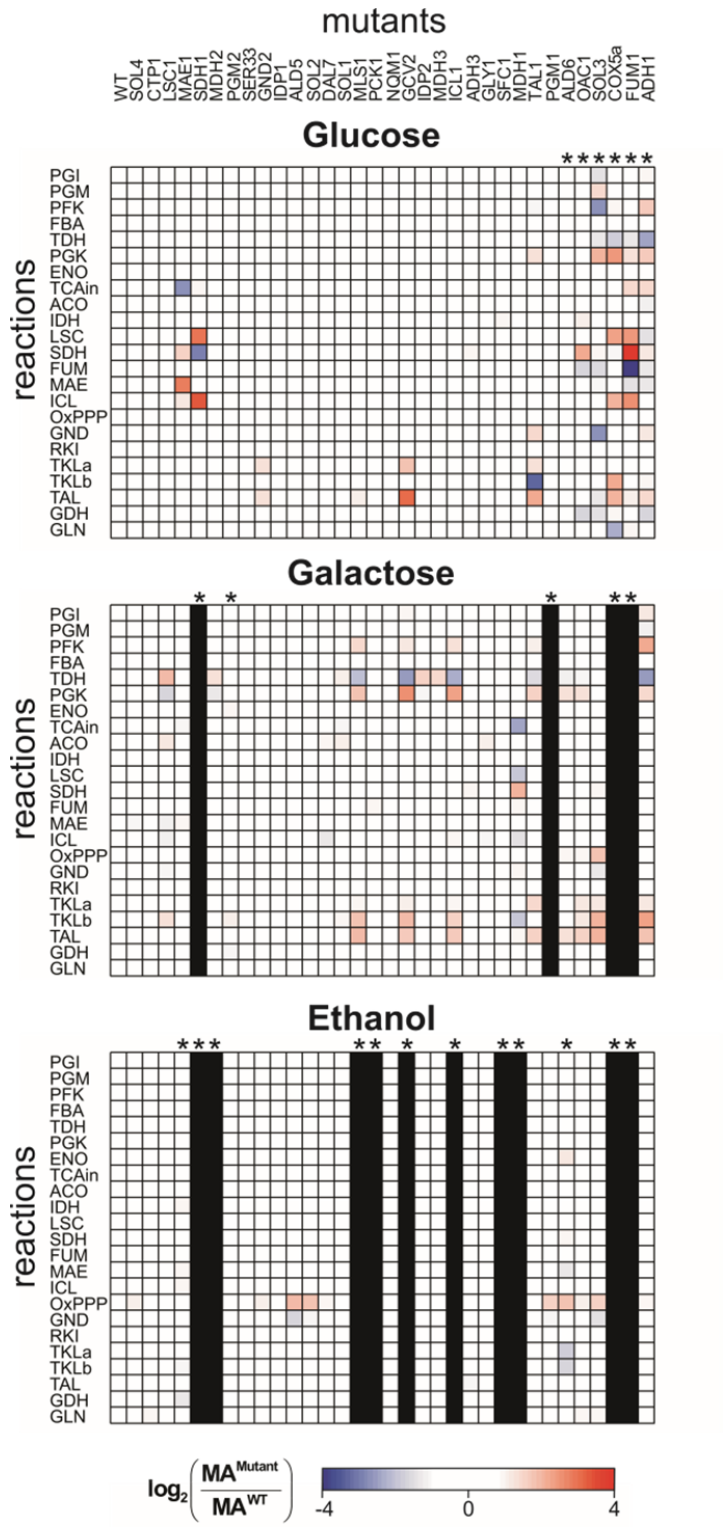
mutants
WT
SOL4
CTP1
LSC1
MAE1
SDH1
MDH2
PGM2
SER33
GND2
IDP1
ALD5
SOL2
DAL7
SOL1
MLS1
PCK1
NQM1
GCV2
IDP2
MDH3
ICL1
ADH3
GLY1
SFC1
MDH1
TAL1
PGM1
ALD6
OAC1
SOL3
COX5a
FUM1
ADH1
Glucose
Galactose
Ethanol
reactions
PGI
PGM
PFK
FBA
TDH
PGK
ENO
TCAin
ACO
IDH
LSC
SDH
FUM
MAE
ICL
OxPPP
GND
RKI
TKLa
TKLb
TAL
GDH
GLN
log2 (MA^Mutant / MA^WT)
-4
0
4

Figure S6: Metabolome response to pentose-phosphate pathway transaldolase deletion

The bars represent relative metabolite concentrations. Absolute quantities can be found in the Supplementary data. Error bars indicate standard deviations calculated from at least four biological replicates. For abbreviations of metabolites refer to Table S2.